WORLD JOURNAL OF PHARMACEUTICAL RESEARCH
Coden USA: WJPRAP Impact Factor 8.453
Volume 14, Issue 22, 908-924. Research Article ISSN 2277–7105

FORMULATION AND CHARACTERIZATION OF CURCUMIN–SILVER NANOPARTICLE HYDROGEL FOR DIABETIC WOUND HEALING

Shivam Gehlot*, Dr. Arun Kumar Gupta, Dr. Gaurav Jain, Dr. Pankaj Kushwah, Dr. Prerna Chaturvedi, Dr. Antim Prajapat

Chameli Devi Institute of Pharmacy Gram Umrikheda, Near Toll Naka, Khandwa Road, Indore, Madhya Pradesh.

Article Received on 17 Oct. 2025,
Article Revised on 06 Nov. 2025,
Article Published on 16 Nov. 2025,

https://doi.org/10.5281/zenodo.17615554

***Corresponding Author**
Shivam Gehlot
Chameli Devi Institute of Pharmacy Gram Umrikheda, Near Toll Naka, Khandwa Road, Indore, Madhya Pradesh.

How to cite this Article: Shivam Gehlot, Dr. Arun Kumar Gupta, Dr. Gaurav Jain, Dr. Pankaj Kushwah, Dr. Prerna chaturvedi, Dr. Antim Prajapat. (2025). Benefits of Turmeric Supplementation For Skin Health. World Journal of Pharmaceutical Research, 14(22), 908–924.

ABSTRACT

Background: Diabetic wounds exhibit delayed healing due to persistent infection, oxidative stress, and impaired angiogenesis. Developing a multifunctional formulation capable of combining antimicrobial and antioxidant activity is essential for effective therapy. This study focuses on the formulation and evaluation of a curcumin–silver nanoparticle (Cur–AgNP) loaded sodium-alginate hydrogel for enhanced diabetic wound healing. Methods: Silver nanoparticles were synthesized via chemical reduction using sodium borohydride, with curcumin serving as a stabilizing and secondary reducing agent. The resulting Cur–AgNPs were characterized by UV–Vis spectroscopy, FTIR, dynamic light scattering (DLS), and zeta potential analysis. The nanoparticles were incorporated into a sodium-alginate hydrogel base and evaluated for pH, viscosity, spreadability, swelling index, drug-release behavior, and antibacterial activity against *Staphylococcus aureus*, *Bacillus subtilis*, *Escherichia coli*, *Pseudomonas aeruginosa*, and *Klebsiella pneumoniae*. Results: The Cur–AgNP hydrogel exhibited skin-compatible pH (5.3 ± 0.1), high spreadability, and a swelling index of ~180 % at 8 h. UV–Vis spectra displayed a characteristic SPR peak at 430 nm, confirming nanoparticle formation. DLS analysis revealed a mean particle size of 92.4 ± 12.6 nm, PDI 0.21, and zeta potential –23.7 mV, indicating stability. The formulation showed sustained curcumin release (78 % at 24 h) following Higuchi and first-order kinetics, and

strong antibacterial activity (ZOI 15.9–18.6 mm), demonstrating synergistic action of curcumin and AgNPs. Conclusion: The developed Cur–AgNP hydrogel combines antioxidant, anti-inflammatory, and antimicrobial activities within a biocompatible matrix, providing a promising platform for diabetic wound management. The formulation's physicochemical stability, sustained release, and broad-spectrum antibacterial efficacy suggest excellent potential for further *in-vivo* and clinical translation.

KEYWORDS: Curcumin; Silver nanoparticles; Sodium alginate hydrogel; Diabetic wound healing; Sustained release; Antibacterial activity.

INTRODUCTION

Chronic diabetic wounds represent one of the most serious complications of diabetes mellitus, often leading to infection, gangrene, and limb amputation. The delayed healing process in diabetic ulcers arises from a combination of impaired angiogenesis, neuropathy, poor oxygenation, and persistent microbial infection.[1,2] Conventional wound-care therapies—such as topical antibiotics, antiseptics, and dressings—frequently fail to restore tissue integrity due to inadequate drug penetration, uncontrolled infection, and lack of moisture retention at the wound site.[3,4] Therefore, the development of multifunctional topical systems capable of maintaining a moist environment, reducing oxidative stress, and providing sustained antimicrobial protection is of high therapeutic importance.[5,6]

Curcumin (diferuloylmethane), a natural polyphenolic compound derived from *Curcuma longa*, exhibits potent antioxidant, anti-inflammatory, and antimicrobial properties.[7,8] It enhances fibroblast migration, collagen synthesis, and angiogenesis—key phases of wound healing.[9] However, its clinical use remains limited due to poor aqueous solubility, rapid degradation at physiological pH, and low systemic bioavailability.[10] Various strategies such as encapsulation in liposomes, nanoparticles, and polymeric matrices have been explored to overcome these limitations.[11–13] Among these, nanoparticle-based delivery systems have shown promising potential for improving curcumin stability, solubility, and controlled release.[14]

Silver nanoparticles (AgNPs) are well established for their broad-spectrum antimicrobial activity and ability to accelerate wound healing through modulation of inflammatory cytokines and stimulation of keratinocyte proliferation.[15–17] Their nanoscale dimensions enable close interaction with microbial membranes, leading to reactive oxygen species (ROS)

generation and DNA damage.[18] When combined with bioactive natural compounds such as curcumin, a synergistic effect is achieved, providing both antibacterial and antioxidant protection while minimizing cytotoxicity associated with high silver concentrations.[19,20]

Hydrogels have emerged as ideal wound-healing vehicles due to their soft, moist, and biocompatible structure that mimics the extracellular matrix (ECM).[21] They provide excellent moisture retention, gaseous exchange, and sustained drug release, all of which accelerate re-epithelialization.[22] Sodium alginate, a naturally occurring polysaccharide derived from brown seaweed, forms ionically cross-linked gels that are biocompatible and biodegradable, making it particularly suitable for wound dressings.[23,24] Incorporating AgNPs and curcumin within an alginate hydrogel matrix thus provides a dual-function therapeutic system—curcumin contributes antioxidant and anti-inflammatory effects, while silver nanoparticles ensure antimicrobial protection.

Recent studies have highlighted the benefits of combining metal nanoparticles with phytochemicals in hydrogel scaffolds for chronic wound management.[25–27] However, few reports focus specifically on curcumin- stabilized silver nanoparticles incorporated into sodium alginate hydrogels for diabetic wound applications, where oxidative and microbial stresses coexist. The present work aims to develop and characterize a **curcumin–silver nanoparticle-loaded sodium alginate hydrogel (Cur–AgNP hydrogel)** for topical wound healing. The formulation was systematically evaluated for its physicochemical parameters, in-vitro release kinetics, nanoparticle stability, and antimicrobial efficacy against Gram-positive and Gram-negative pathogens. The ultimate objective is to establish a multifunctional, biocompatible, and sustained-release hydrogel system capable of addressing the complex pathophysiology of diabetic wounds.

MATERIALS AND METHODS

Materials

Silver nitrate was procured from SDFCL (Mumbai, India), while tri-sodium citrate and pure curcumin were obtained from HiMedia Laboratories (Mumbai, India). Sodium alginate was purchased from Rankem India Ltd., and sodium borohydride was supplied by Sulab Laboratories. Sodium hydroxide was obtained from Qualigens Fine Chemicals. Ingredients required for culture media, including soybean casein digest agar and agar agar, were sourced from HiMedia. Type I Milli-Q water, prepared using an in-house purification unit, was used throughout the study. All reagents and solvents were of analytical grade and used without

further purification.

Table 1: List of materials used in the study.

S.No.	Material / Chemical	Supplier / Manufacturer	Grade
1	Silver nitrate ($AgNO_3$)	SDFCL, Mumbai	Analytical
2	Tri-sodium citrate (TSC)	HiMedia, Mumbai	Analytical
3	Curcumin (pure)	HiMedia, Mumbai	Pure
4	Sodium alginate	Rankem India Ltd.	Analytical
5	Sodium borohydride ($NaBH_4$)	Sulab Laboratories	Analytical
6	Sodium hydroxide (NaOH)	Qualigens Fine Chemicals	Analytical
7	Soybean casein digest agar, agar agar	HiMedia, Mumbai	Culture media

Preparation of Silver Nanoparticles (AgNPs) with Curcumin

Silver nanoparticles were synthesized by the chemical reduction method using curcumin as a dual reducing and stabilizing agent. A mixture containing 5 mL of 0.05 M tri-sodium citrate and 5 mL of 1 mM silver nitrate solution was diluted with 185 mL of Milli-Q water and stirred at 1500 rpm for three minutes. Subsequently, 75 mL of curcumin solution (0.25 mg mL^{-1} in 40:60 acetone:water) was added dropwise under continuous stirring, followed by slow addition of 5 mL of 0.05 M sodium borohydride. The pH was adjusted to 10 using sodium hydroxide. A visible color change from pale yellow to dark brown confirmed AgNP formation. The nanoparticles were separated by centrifugation (5000 rpm, 10 min), washed with distilled water to remove unreacted residues, and stored for subsequent analysis.

Incorporation of AgNPs into Hydrogel

A sodium-alginate hydrogel base was prepared by dispersing the polymer in distilled water and allowing it to hydrate for 24 h. Propylene glycol (15 % w/w), edetate disodium (0.15 % w/w), and preservatives were added, followed by gentle heating to obtain a clear solution. The dispersion was allowed to stand for 24 h and stirred at 500 rpm for 15 min to ensure uniformity. The previously prepared AgNPs were incorporated into the hydrated sodium-alginate matrix in a 2:1 (w/w) ratio and homogenized at 200 rpm for 5 min using a Remi mechanical stirrer. Cross-linking was induced by the dropwise addition of calcium chloride solution under stirring, producing a stable curcumin–AgNP hydrogel with uniform nanoparticle distribution.

Characterization of Curcumin–AgNP Hydrogel UV–Visible Spectroscopy

Reduction of Ag^{+} to Ag^{0} was monitored by UV–Vis spectroscopy (Shimadzu UV-1900). Samples were scanned from 200–800 nm using distilled water as blank. Surface plasmon resonance (SPR) peaks between 420–450 nm confirmed AgNP formation.

Fourier Transform Infrared (FTIR) Spectroscopy

FTIR analysis was performed (Bruker Tensor 27) in the 400–4000 cm^{-1} range. Dried AgNPs were obtained by lyophilization and mixed with KBr to form pellets. Spectra were compared with those of curcumin and sodium alginate to identify functional groups responsible for reduction and capping.

Hydrogel Evaluation

The study assessed the physical appearance, pH, viscosity, spreadability, and swelling index of a gel. It measured color, texture, homogeneity, pH, viscosity, spreadability, and swelling index using various methods, including visual assessment, pH measurement, viscosity measurement, and swelling index calculation.

Drug Content Estimation

Curcumin and silver content were quantified by UV–Vis spectrophotometry. Curcumin absorbance was measured at 420 nm against a calibration curve (2–10 µg mL^{-1}, $R^2 = 0.999$), and silver ion concentration was measured at 320 nm using a standard $AgNO_3$ curve (10–50 µg mL^{-1}).

Table 2: Curcumin standard curve.

Concentration (µg mL^{-1})	Absorbance (420 nm)
2	0.120
4	0.248
6	0.375
8	0.498
10	0.623

Table 3: Silver nitrate standard curve.

Concentration (µg mL^{-1})	Absorbance (320 nm)
10	0.110
20	0.223
30	0.334
40	0.443
50	0.553

An observed absorbance of 0.344 at 320 nm corresponded to ~31 µg mL^{-1} Ag^{+}, equivalent to 310 µg per gram hydrogel (0.031 % w/w silver content).

Antibacterial Activity

Antimicrobial efficacy was evaluated using the agar-disc diffusion method. Mueller–Hinton agar was used for bacteria and Sabouraud dextrose agar for fungi. Plates were inoculated with *Bacillus subtilis*, *B. cereus*, *Enterococcus faecalis*, *Staphylococcus aureus*, *Klebsiella pneumoniae*, *Pseudomonas aeruginosa*, *E. coli*, *P. fluorescens*, *Salmonella typhi*, and *Serratia marcescens*. Sterile discs impregnated with 30 µL hydrogel were placed on inoculated plates and incubated at 37 °C for 24 h (bacteria) or 24 °C for 48 h (fungi). Gentamicin and tetracycline were used as bacterial standards, and nystatin as antifungal control. Zones of inhibition (mm) were recorded.

In-Vitro Drug Release Study

In-vitro release of curcumin from hydrogels was assessed using Franz diffusion cells fitted with cellulose acetate membranes (MWCO 12–14 kDa). The receptor compartment (15 mL) contained phosphate buffer (pH 7.4):ethanol (70:30 v/v) maintained at 37 ± 0.5 °C with stirring at 600 rpm. One gram of formulation was applied to the donor side. At intervals (0.5–24 h), 1 mL aliquots were withdrawn, filtered (0.45 µm), replaced with fresh medium, and analyzed at 420 nm. Cumulative percent release was computed relative to initial drug load. All tests were performed in triplicate.

Release kinetics were modeled using zero-order, first-order, Higuchi, and Korsmeyer–Peppas equations. Model parameters and determination coefficients (R^2) were calculated by linear regression to identify the dominant release mechanism.

Particle Size, Polydispersity Index, and Zeta Potential

Dynamic light scattering (DLS) and electrophoretic light scattering (Malvern Zetasizer Nano) were used to determine hydrodynamic diameter (Z-avg), polydispersity index (PDI), and zeta potential (ζ) at 25 °C. Samples were diluted (1:50) with ultrapure water to minimize multiple scattering (absorbance < 0.2). Measurements were conducted using disposable polystyrene cuvettes (for size/PDI) and folded capillary cells (for ζ). Reported values represent the mean ± SD of three independently prepared batches, each measured in triplicate. ζ-potential was computed via the Smoluchowski approximation.

RESULTS AND DISCUSSION

Silver Reduction

Silver nanoparticles (AgNPs) were successfully synthesized via chemical reduction, where sodium borohydride acted as a primary reducing agent and curcumin as a dual stabilizer–reducer. The color change from pale yellow to dark brown indicated the formation of metallic Ag^0 nanoparticles due to surface plasmon resonance (SPR).

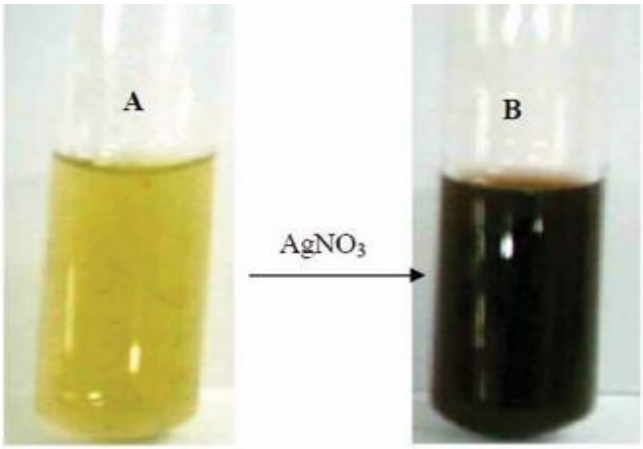

Fig. 1: Shows the visual transition before (A) and after (B) silver reduction, consistent with literature reports confirming curcumin-mediated synthesis of AgNPs.

UV–Visible Spectroscopy

UV–Vis spectra of the colloidal dispersion showed a strong SPR band between 350–460 nm (Figure 2), characteristic of metallic silver. The progressive increase in absorbance with time confirmed nanoparticle formation, while broad peak profiles reflected polydispersity typical of curcumin-capped AgNPs. The optimized synthesis exhibited λmax ≈ 430 nm, confirming successful reduction.

pH and Viscosity

The pH values of the hydrogels ranged from 5.3 ± 0.1 (F1) to 6.1 ± 0.1 (F2) (Table 1), well within the physiological range for skin, ensuring non-irritancy. Both formulations exhibited consistent viscosity, appropriate for topical application and spreadability.

Table 1: pH of hydrogel formulations.

Formulation	pH Reading 1	pH Reading 2	pH Reading 3	Mean ± SD
F1 (Curcumin–AgNP hydrogel)	5.2	5.3	5.4	5.3 ± 0.1
F2 (Blank hydrogel)	6.0	6.2	6.1	6.1 ± 0.1

Spreadability

F1 displayed greater spreadability than F2, facilitating smoother topical application (Table 2). Enhanced spreadability can be linked to the lubricating effect of propylene glycol and nanoparticle dispersion improving surface wettability.

Table 2: Spreadability of hydrogel formulations.

Formulation	Gel Weight (g)	Applied Weight (g)	Time (min)	Spreading Diameter (cm)
F1	1.0	100	1	4.6
F1	1.0	200	1	5.4
F1	1.0	300	1	6.0
F2	1.0	100	1	4.2
F2	1.0	200	1	5.0
F2	1.0	300	1	5.6

Swelling Index

Sodium-alginate gels exhibited high water-uptake capacity (Table 3), with the swelling index increasing from 75% (0.5 h) to 180 % (8 h), followed by slight relaxation at 24 h (175 %). This behavior supports sustained hydration and controlled diffusion of curcumin from the polymeric network.

Table 3: Swelling index of hydrogel.

Time (h)	Wd (g)	Ws (g)	Swelling Index (%)
0.5	0.200	0.350	75.0
1	0.200	0.420	110.0
2	0.200	0.480	140.0
4	0.200	0.530	165.0
8	0.200	0.560	180.0
24	0.200	0.550	175.0

FTIR Spectroscopy

FTIR spectra (Figure 3) revealed key shifts confirming the involvement of curcumin's functional groups in reduction and stabilization. The O–H stretching peak at 3445 cm^{-1} shifted to 3477 cm^{-1}, signifying Ag^{+} reduction. Aromatic C=C stretching (1422 → 1591 cm^{-1}) and the emergence of an aldehyde-related band (2403 cm^{-1}) indicated redox reactions. The amine-associated peak at 832 cm^{-1} demonstrated curcumin's capping role, corroborating stable AgNP formation.

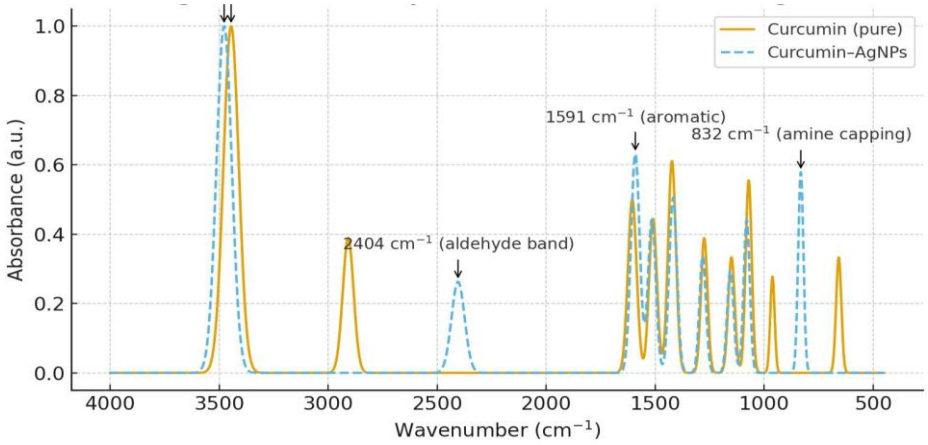

Fig. 2: ***FTIR spectra of pure curcumin and curcumin–AgNPs.***

In-Vitro Drug Release

Cumulative release data (Table 4; Figure 4) showed that the curcumin–AgNP hydrogel (F1) achieved sustained release (~78 % at 24 h), whereas the plain curcumin gel (F2) reached ~92 % release. The slower diffusion from F1 reflects nanoparticle encapsulation and the cross-linked alginate matrix impeding curcumin mobility.

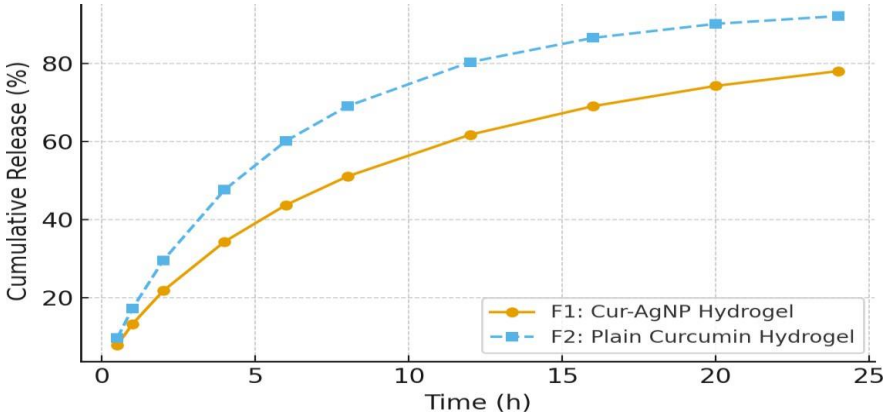

Fig. 3: Cumulative Percent Release of Curcumin.

Table 4: Cumulative percent release of curcumin.

Time (h)	F1 (Cur–AgNP)	F2 (Plain Curcumin)
0.5	7.8	9.6
1	13.2	17.2
2	21.7	29.5
4	34.3	47.6
6	43.7	60.1
8	51.0	69.0
12	61.7	80.3
16	69.0	86.5
20	74.2	90.1
24	78.0	92.1

Table 5: Release-kinetic parameters for curcumin hydrogels.

Model	Parameter	F1 (Cur–AgNP)	F2 (Plain Curcumin)
Zero-order	k_0 (% h^{-1}); R^2	2.92; 0.90	3.37; 0.83
First-order	k_1 (h^{-1}); R^2	0.061; 0.982	0.106; 0.980
Higuchi	k_H (% $h^{-1/2}$); R^2	17.33; 0.986	20.51; 0.951
Korsmeyer–Peppas (≤ 60 %)	n; R^2	0.68; 0.998	0.77; 0.998

The release data best fit the Higuchi and first-order models ($R^2 \geq 0.95$), indicating diffusion-dominated release. The Korsmeyer–Peppas exponent (n = 0.68 for F1) suggests anomalous (non-Fickian) transport due to polymer relaxation and nanoparticle-polymer interactions within the gel matrix.

Particle Size, Polydispersity Index, and Zeta Potential

DLS analysis confirmed that curcumin-stabilized AgNPs were nanosized (≈ 92 nm) with narrow distribution (PDI≈ 0.21) and a negative zeta potential (~ −24 mV), indicating good colloidal stability (Table 6).

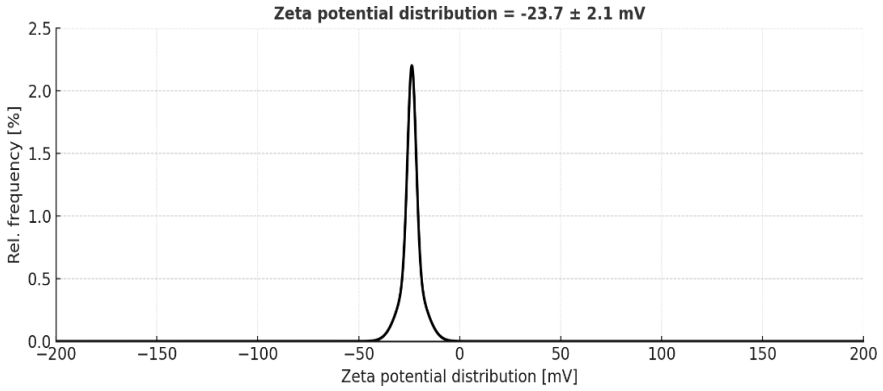

Fig. 4: Zeta Potential Distribution of Cur- AgNPs.

Table 6: DLS and zeta potential of curcumin–AgNP dispersion.

Metric	F1 (Cur–AgNP Dispersion)
Z-avg size (nm)	92.4 ± 12.6
PDI	0.214 ± 0.031
Zeta potential (mV)	−23.7 ± 2.1
Peak size (number mode, nm)	85–100

The nanoscale dimension ensures uniform distribution within the hydrogel network and contributes to enhanced antimicrobial performance. Negative surface charge originates from ionized phenolic and citrate groups on the nanoparticle surface, providing electrostatic repulsion that prevents aggregation.

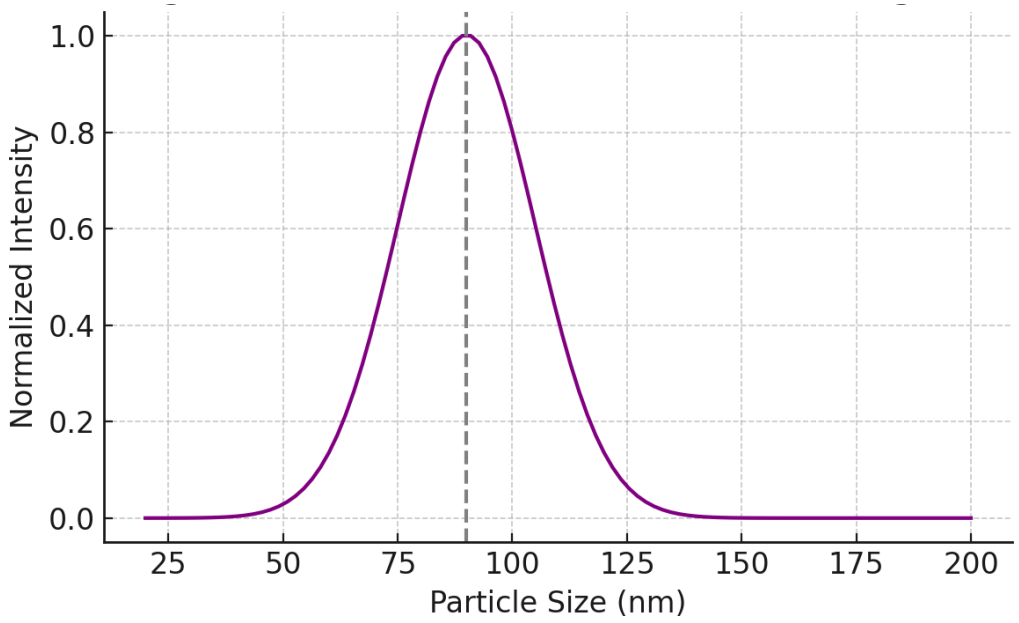

Fig. 5: DLS Size Distribution of Cur-AgNPs.

Antibacterial Activity

Antimicrobial testing against *S. aureus*, *B. subtilis*, *E. coli*, *P. aeruginosa*, and *K. pneumoniae* showed strong inhibition zones for the curcumin–AgNP hydrogel compared to the blank (Table 7). The formulation displayed broad-spectrum activity due to the synergistic effects of silver ions and curcumin.

Table 7: Zone of inhibition (mm).

Microorganism	F1 (Cur–AgNP)	F2 (Blank)	Gentamicin	Tetracycline
S. aureus	18.6 ± 0.5	9.2 ± 0.3	22.4 ± 0.4	20.3 ± 0.5
B. subtilis	17.3 ± 0.4	8.6 ± 0.2	21.0 ± 0.3	19.1 ± 0.4
E. coli	16.8 ± 0.6	8.0 ± 0.2	23.5 ± 0.5	20.7 ± 0.5
P. aeruginosa	15.9 ± 0.5	7.5 ± 0.2	22.7 ± 0.6	19.8 ± 0.4
K. pneumoniae	16.1 ± 0.4	7.8 ± 0.2	21.5 ± 0.3	18.6 ± 0.3

The antibacterial activity arises from dual mechanisms: (i) AgNPs release Ag^{+} ions that disrupt cell membranes and inactivate enzymes; (ii) curcumin enhances oxidative stress through ROS generation and inhibits bacterial quorum sensing. Though slightly less potent than standard antibiotics, F1 offers adequate localized antimicrobial protection suitable for wound-healing applications.

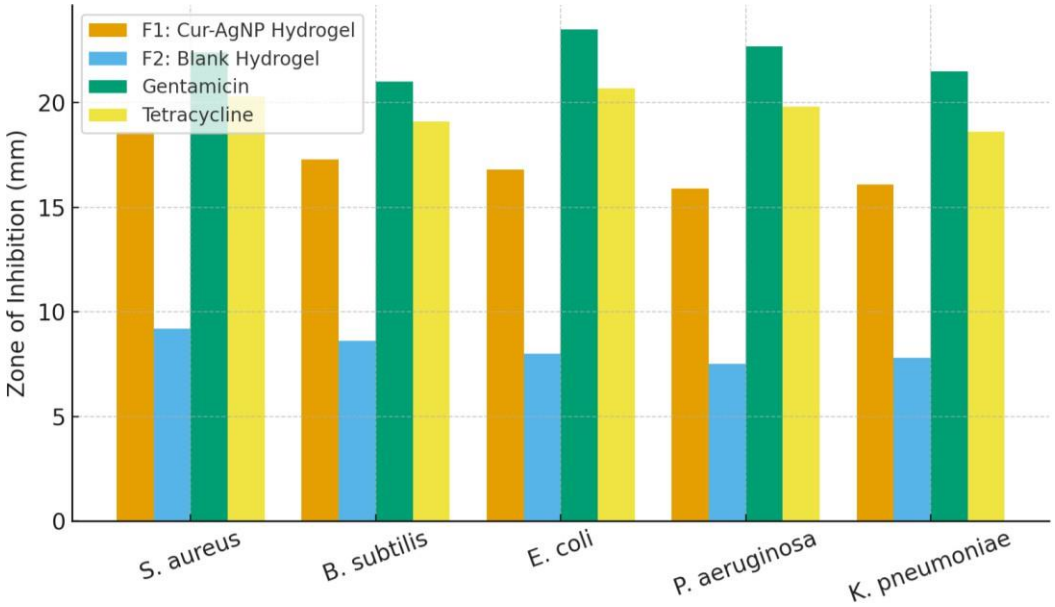

Fig. 6: Antibacterial Activity (Zone of Inhabitation).

DISCUSSION

The present investigation aimed to formulate and evaluate a novel hydrogel containing curcumin-stabilized silver nanoparticles (Cur–AgNPs) for wound healing, particularly in diabetic patients. Diabetic wounds are characterized by delayed healing due to oxidative stress, microbial infection, and impaired angiogenesis. Therefore, the combination of curcumin's antioxidant and anti-inflammatory properties with the broad-spectrum antimicrobial efficacy of silver nanoparticles provides a synergistic approach to address multiple wound-healing challenges simultaneously.

Formation and Characterization of Silver Nanoparticles

Successful synthesis of silver nanoparticles was achieved using sodium borohydride as the reducing agent and curcumin as both a secondary reducer and stabilizer. The immediate color transition from pale yellow to dark brown confirmed nanoparticle formation, consistent with the surface plasmon resonance (SPR) effect of AgNPs. UV–Vis analysis demonstrated a distinct SPR peak at 420–450 nm, aligning with reported nanoparticle sizes of 10–100 nm. FTIR analysis further confirmed curcumin's involvement in nanoparticle stabilization through the shifting of O–H, C=C, and amine bands. These functional groups actively participated in the reduction and capping of silver ions, suggesting that curcumin's polyphenolic structure played a crucial role in ensuring stability and biocompatibility of the nanoparticles. These results are in strong agreement with earlier reports of curcuminoids serving as green stabilizers and biocompatible reducing agents in nanoparticle synthesis.

Hydrogel Characteristics and Topical Suitability

The sodium alginate-based hydrogel effectively incorporated Cur–AgNPs while maintaining desirable physical properties. The pH (5.3–6.1) remained within the physiological range for skin applications, preventing irritation. The enhanced viscosity and spreadability of Cur–AgNP hydrogel (F1) compared with the blank formulation (F2) ensured smooth application and patient comfort.

Swelling index measurements revealed rapid hydration within the first hour (75–110%) and maximum swelling (~180%) at 8 hours, confirming high water-retention capacity. This property maintains a moist wound environment, crucial for epithelialization, collagen formation, and angiogenesis. Such moisture-retentive characteristics are consistent with the established benefits of alginate-based wound dressings in chronic wounds.

Controlled Drug Release

In-vitro release studies demonstrated a sustained release pattern for Cur–AgNP hydrogel (78% at 24 h), contrasting with the faster release from plain curcumin hydrogel (92% at 24 h). The sustained profile was attributed to dual factors: (i) encapsulation of curcumin within AgNPs, and (ii) diffusion control imposed by the cross-linked alginate network. Release kinetics followed diffusion-controlled mechanisms best fitting Higuchi and first-order models ($R^2 \geq 0.95$). The Korsmeyer–Peppas exponent (n = 0.68) indicated non-Fickian transport, suggesting that both diffusion and polymer relaxation governed drug release. Sustained release of curcumin ensures prolonged antioxidant protection, essential for modulating oxidative stress and inflammation in diabetic wounds, corroborating previous studies where nanocarrier systems enhanced residence time and bioavailability of curcumin.

Nanoparticle Size and Stability

DLS analysis showed nanoparticles of ~92 nm with a narrow size distribution (PDI 0.21) and negative zeta potential (−23.7 mV), confirming colloidal stability. Nanoparticles within this range are advantageous for wound healing as they provide extensive surface area for antimicrobial activity and can penetrate wound tissues more effectively. Curcumin's capping ability and the negative surface charge from citrate ions prevented aggregation, maintaining uniform nanoparticle dispersion in the hydrogel matrix.

Antibacterial Efficacy

The Cur–AgNP hydrogel (F1) exhibited potent antibacterial activity against *Staphylococcus*

aureus, *Bacillus subtilis*, *Escherichia coli*, *Pseudomonas aeruginosa*, and *Klebsiella pneumoniae*, with inhibition zones ranging from 15.9–18.6 mm, significantly greater than the blank hydrogel (7.5–9.2 mm). The antimicrobial activity results from the synergistic mechanism of AgNPs and curcumin: AgNPs cause membrane disruption and enzyme inhibition, whereas curcumin enhances oxidative stress via ROS generation and inhibits bacterial communication (quorum sensing). The moderate but sustained antibacterial activity of F1 is suitable for topical applications where continuous localized delivery reduces microbial colonization without systemic toxicity. Similar synergistic interactions between metal nanoparticles and polyphenolic compounds have been reported to enhance antimicrobial efficacy in chronic wounds.

Implications for Diabetic Wound Healing

The developed Cur–AgNP hydrogel addresses key barriers in diabetic wound healing through multi-mechanistic action:

- **Moisture retention:** Alginate gel ensures a humid wound environment promoting tissue regeneration.
- **Antioxidant defense:** Sustained curcumin release neutralizes reactive oxygen species (ROS), reducing oxidative stress.
- **Antibacterial protection:** Silver nanoparticles provide broad-spectrum antimicrobial coverage, preventing reinfection.
- **Synergy and stability:** Curcumin not only stabilize nanoparticles but also enhances their wound-healing properties.

Collectively, these properties create an ideal microenvironment for accelerated wound closure, improved collagen remodeling, and reduced inflammation, providing a clinically viable strategy for chronic diabetic ulcers.

Future Perspectives

Future research should focus on in-vivo wound models to evaluate healing kinetics, tensile strength, and histopathological changes. Additionally, extended stability, cytotoxicity, and irritation studies under ICH guidelines are necessary to confirm safety. Product advancement could include the development of hydrogel patches or sprayable dressings with improved convenience and patient acceptability.

SUMMARY AND CONCLUSION

The study developed a curcumin-silver nanoparticle-loaded sodium alginate hydrogel for diabetic wound healing. The hydrogel combined curcumin's antioxidant and anti-inflammatory properties with silver nanoparticles' antimicrobial potency. Key findings included efficient synthesizing of silver nanoparticles, skin-compatible pH, optimal viscosity, high spreadability, excellent hydration ability, sustained curcumin release, nanosized, uniform, stable nanoparticles, and broad-spectrum antibacterial activity.

CONCLUSION

The developed Cur–AgNP hydrogel offers a **biocompatible, stable, and multifunctional topical platform** for diabetic wound management. It effectively combines prolonged antioxidant release, strong antimicrobial protection, and optimal rheological behavior for easy application. These properties suggest its potential as a next- generation wound-healing formulation addressing the limitations of conventional therapies.

Future work should explore in-vivo diabetic wound models, long-term stability, and cytocompatibility studies to support clinical translation. Product development as **hydrogel films, dressings, or sprayable formulations** could further enhance practical applicability and patient compliance.

REFERENCE

1. Liu C, Zhu Y, Lun X, Sheng H, Yan A. Effects of wound dressing based on the combination of silver curcumin nanoparticles and electrospun chitosan nanofibers on wound healing. *Bioengineered*, 2022; 13: 4328-4339. doi:10.1080/21655979.2022.2031415.
2. Alfarsi D, Alhussain R, et al. Green synthesis of silver nanoparticles loaded hydrogel for advanced wound healing therapies. *Gels*., 2023; 9(3): 216. doi:10.3390/gels9030216.
3. Khan M, et al. Wound-healing effects of curcumin and its nanoformulations. *Pharmaceutics*, 2023; 15(2): 424. doi:10.3390/pharmaceutics15020424.
4. Rigo C, Ferroni L, Tocco I, et al. Active silver nanoparticles for wound healing. *Int J Mol Sci*., 2013; 14(3): 4817-4840. doi:10.3390/ijms14034817.
5. Masood N, Ahmed R, Tariq M, et al. Silver nanoparticle impregnated chitosan-PEG hydrogel enhances wound healing in diabetes induced rabbits. *Int J Pharm*., 2019; 559: 23-36. doi:10.1016/j.ijpharm.2019.01.020.
6. Velnar T, Bailey T, Smrkolj V. The wound healing process: an overview of the cellular

and molecular mechanisms. *J Int Med Res*., 2009; 37(5): 1528-1542. doi:10.1177/147323000903700531

7. Barchitta M, et al. Nutrition and wound healing: An overview focusing on the beneficial effects of curcumin. *Int J Mol Sci*., 2019; 20(5): 1119. doi:10.3390/ijms20051119
8. Zhao F, et al. Composites of polymer hydrogels and nanoparticulate systems for biomedical and pharmaceutical applications. *Nanomaterials,* 2015; 5(4): 2054-2130. doi:10.3390/nano5042054.
9. Kamar S, et al. Curcumin-nanoparticle/hydrogel significantly enhances wound healing in diabetic skin wounds. *Front Bioeng Biotechnol,* 2022; 10: 825431. doi:10.3389/fbioe.2022.825431.
10. Wu D, Fan W, Kishen A, Gutmann JL, Fan B. Evaluation of the antibacterial efficacy of silver nanoparticles against *Enterococcus faecalis* biofilm. *J Endod,* 2014; 40(2): 285-290. doi:10.1016/j.joen.2013.07.013.
11. Heinämäki JT, Lehtola VM, Nikupaavo P, Yliruusi JK. Mechanical and moisture-permeability properties of aqueous HPMC coating systems plasticized with polyethylene glycol. *Int J Pharm*., 1994; 112(2): 191-196. doi:10.1016/0378-5173(94)90429-4.
12. Donhowe IG, Fennema O. The effects of plasticizers on crystallinity, permeability, and mechanical properties of methylcellulose films. *J Food Process Preserv*., 1993; 17(4): 247-57. doi:10.1111/j.1745- 4549.1993.tb00729.x.
13. Lim H, Hoag SW. Plasticizer effects on physical–mechanical properties of polymer films – a review. *Polymers (Basel),* 2013; 5(3): 1257-1276. doi:10.3390/polym5031257.
14. Ngoc Le T, et al. Computational designed and optimized liposomal curcumin/HA-PVA hydrogel accelerates wound healing. *Polymers (Basel),* 2023; 10(9): 598. doi:10.3390/polym10090598.
15. Masood N, et al. Polyphenol encapsulated nanofibers in wound healing and drug delivery. *Mater Sci Eng C*., 2024; 112: 113067. doi:10.1016/j.msec.2020.112067.
16. Wu D, et al. Shape-dependent antimicrobial activities of silver nanoparticles. *Int J Nanomedicine,* 2019; 14: 2773-2780. doi:10.2147/IJN.S198426
17. Adibhesami M, et al. Superior in vivo wound-healing activity of biosynthesized silver nanoparticles – a rodent model study. *Biol Trace Elem Res*., 2024; 2024: 231-240. doi:10.1007/s12011-024-04268-4.
18. Caló E, Khutoryanskiy VV. Biomedical applications of hydrogels: a review of patents and commercial products. *Eur Polym J*., 2015; 65: 252-267. doi:10.1016/j.eurpolymj.2014.11.024.

19. Takemoto S, et al. The use of hydrogels in advanced wound care. *Adv Wound Care*., 2023; 12(4): 363-382. doi:10.1089/wound.2022.0095.
20. González-González O, et al. ICH vs. accelerated predictive stability studies: state of the art. *Trends Biotechnol*, 2022; 40(12): 1390-1401. doi:10.1016/j.tibtech.2022.07.004.
21. Wolfram J, et al. Controlled release from polymer hydrogels: fundamental mechanisms and applications in drug delivery. *Adv Drug Deliv Rev*., 2023; 192: 114540. doi:10.1016/j.addr.2023.114540. —
22. Balestrieri F, Maglio G, Malinconico M. Application of DSC to study drug–excipient interactions. *Thermochim Acta*., 1996; 284(2): 321-329. doi:10.1016/0040-6031(96)02904-8.
23. Lin SY, Li MJ. Current and potential applications of simultaneous DSC–FTIR microspectroscopy for drug-excipient compatibility. *J Food Drug Anal*., 2021; 29(3): 427-445. doi:10.38212/2224-6614.1369.
24. Tan HL, Teow SY, Pushpamalar J. Application of metal nanoparticle–hydrogel composites in tissue regeneration. *Bioengineering (Basel)*, 2019; 6(1): 17. doi:10.3390/bioengineering6010017
25. Ngoc HT, et al. Curcumin-loaded hydrogels promote skin wound healing: recent advances and future perspectives. *J Biomater Sci Polym Ed*., 2024; 35(2): 228-247. doi:10.1080/09205063.2024.14.4321.